Eur. Phys. J. A (2025) 61:148
https://doi.org/10.1140/epja/s10050-025-01619-0

THE EUROPEAN PHYSICAL JOURNAL A

Regular Article - Experimental Physics

Spectroscopic investigation of ^{54}Cr via α-transfer reaction

Biswajit Das[1,a], A. Kundu[1,b], R. Palit[1,c], P. Dey[1], Vishal Malik[1], U. Garg[2], D. Negi[3], S. R. Laskar[4], Rajkumar Santra[5], S. K. Jadhav[1], B. S. Naidu[1], A. T. Vazhappilly[1]

[1] Department of Nuclear and Atomic Physics, Tata Institute of Fundamental Research, Mumbai 400005, India
[2] Department of Physics and Astronomy, University of Notre Dame, Notre Dame, IN 46556, USA
[3] Department of Physics, Manipal Institute of Technology, Manipal Academy of Higher Education, Manipal 576104, India
[4] Istituto Nazionale di Fisica Nucleare, Sezione di Milano, 20133 Milano, Italy
[5] Variable Energy Cyclotron Centre, 1/AF Bidhan Nagar, Kolkata 700064, India

Received: 22 February 2025 / Accepted: 14 June 2025

Communicated by Robert Janssens

Abstract Low-lying states in ^{54}Cr have been investigated via the α-transfer reaction ^{50}Ti(^{7}Li,t) at a bombarding energy of 20 MeV. The exclusive α-transfer channel is separated from other reaction channels through the appropriate energy gate on the complementary particle, triton. Levels of ^{54}Cr populated exclusively by the α-transfer process could be identified up to $\approx$ 5 MeV excitation energy and angular momentum up to $(8)^+$, by identifying the corresponding known γ-rays. These include multiple low-lying non-yrast 2^+ and 4^+ states, which would otherwise be unfavorable via fusion evaporation reactions. The feeding-subtracted γ-ray yields have been extracted to estimate the population of various excited states through the transfer process. The measured integrated transfer cross sections for all the observed yrast and non-yrast states are compared with Coupled Channels calculations using FRESCO to extract the α+^{50}Ti core spectroscopic factors. For the yrast states, a higher α+core overlap is seen for the 2^+ and 4^+ states, while it is seen to be less favorable for the 6^+ and $(8)^+$ states when α-transfer is considered to occur predominantly as a direct one-step process to the ^{50}Ti core ground state. The yrast 2^+, and 4^+ states are predominantly populated by single-step transfer, while for the states with spin ≥ 5, the possibility of core excitation followed by α-transfer shows a larger α-core overlap. For the non-yrast 0^+, 2^+, and 4^+ states, single-step transfer shows moderate to small α-core overlap. No higher spin non-yrast states are observed.

1 Introduction

Reactions with nuclei characterized by a weak binding and cluster structure, such as ^{6,7}Li and ^{9}Be continue to provide opportunities to study various nuclear structure phenomena and to elucidate new aspects of reaction dynamics [1–4]. Different mechanisms, such as complete fusion channel, incomplete fusion (ICF), and cluster-transfer reaction channels, have been adopted over the years to understand the competing reaction processes in interactions involving these nuclei as projectiles [5]. Exploring nuclear structure studies by incorporating the selectivity of various reaction mechanisms has been known to have a lot of potential. In this connection, it is important to identify the difference in the population of states of the same residual nucleus using compound-nucleus and direct reaction modes with the same target projectile combination. While ICF reactions, particularly those induced by a ^{7}Li projectile [6–11], have often been used for γ-ray spectroscopy studies of stable and neutron-rich nuclei, the cluster transfer reactions are somewhat less explored for spectroscopic investigations. In this context, the particle-γ coincidence technique presents significant utility. Here, measuring the ejected particle moving with scattered velocity provides information about the excitation energy of the residual nucleus, while the corresponding γ-transitions carry signatures of the excitation and the decay path of the different levels. In particular, a cluster transfer reaction with a large positive Q-value is favorable as one will be able to kinematically separate the ICF/^{6,7}Li breakup channel from the $\alpha/d/t$ transfer channel by measuring the ejectile energy. Recently, such an experiment was carried out at REX-ISOLDE to investigate n-rich nuclei produced via α and t cluster-transfer reactions in inverse kinematics with ^{98}Rb radioactive beam and ^{7}Li target [12]. However, no distinction could be achieved among

[a] e-mail: biswajit.das@tifr.res.in
[b] e-mail: ananyak.delhi@gmail.com
[c] e-mail: palit@tifr.res.in (corresponding author)

Published online: 26 June 2025

t and α particles produced by the direct transfer process and those arising from the elastic breakup-ICF process, with the contribution from the latter, expected to be around 20%. In such measurements, the choice of appropriate kinetic-energy cut on the ejectile spectrum will restrict the reaction channel to one where an isotope is populated exclusively by transfer reaction, without any contribution from particle evaporation or ICF. Besides the high angular momentum yrast states, such reactions can also selectively populate the non-yrast states relevant for nuclear structure investigations. This has been demonstrated in the present work on the ^{50}Ti(^{7}Li,t) system where the outgoing t after α-transfer will have access to the reaction Q-value, unlike those produced by breakup of ^{7}Li.

Another aspect of cluster-transfer reactions with ^{6,7}Li projectiles are the use of their α-transfer component to probe α + core structure in light- and medium-mass nuclei [13–20]. Alpha clustering in sd- and lower fp-shell nuclei is also crucial for comprehending the structural development of light to medium-mass nuclei. Within the sd-shell region (mass number $A \approx 16$–40), nuclei such as ^{20}Ne [21–23], ^{24}Mg [24], ^{28}Si [25], and ^{32}S [26,27] display prominent evidence of alpha clustering. These nuclei frequently exhibit rotational band structures that can be interpreted as arising from alpha plus core configurations; for example, ^{20}Ne can be described as an alpha particle coupled to a ^{16}O core. Conversely, alpha clustering in lower fp-shell nuclei ($A \approx 40$–60), such as ^{44}Ti [28], ^{48}Cr [29], and ^{54}Cr [30], is generally more subtle and complex. Within this mass region, experimental observations indicate the presence of α+ core configurations-for instance, ^{44}Ti can be represented as α+^{40}Ca, and ^{54}Cr as α+^{50}Ti-particularly at moderate excitation energies. However, the expression of clustering phenomena is less evident here due to the increased level density of shell-model configurations and the dominance of stronger mean-field effects. Therefore, key open questions in this area include quantifying the α + core overlap in these states in neutron-rich sd/fp-shell nuclei.

Transfer reactions using ^{6}Li projectile have been used to extract the α spectroscopic factors of ^{40}Ca, ^{44}Ti and ^{94}Mo [28,31]. Fulbright et al. [30] performed the (^{6}Li,d) reaction on a ^{50}Ti target with beam energy of 28–38 MeV and populated the excited states up to 3.5 MeV in ^{54}Cr. Recently, M. A. Souza and H. Miyake [32] have shown the comparison of Q-values for α-separation per nucleon (Q_α/A) for even-mass Cr isotopes as well as A = 46, 54, 56 and 58 isobars, and suggested that ^{46}Cr and ^{54}Cr are the isotopes expected to most favorable for the α + core configuration. Therefore, owing to the availability of stable projectile-target combinations for populating ^{54}Cr via α-transfer, a fresh experimental study for the investigation of the states with α + core configuration and to extract the corresponding spectroscopic factors in ^{54}Cr nucleus is of interest. In nuclear α-transfer reactions, states with an α + core configuration can be populated either through a single-step α-transfer or via a two-step transfer process [33]. In single-step α-transfer, the α particle is directly transferred from the projectile to the target nucleus in one g.s. to g.s. transfer. This process, controlled by angular momentum and parity conservation, mainly favors the population of states with natural parity in the resulting nucleus. On the other hand, two-step alpha transfer proceeds through an intermediate stage, which may involve excitation of either the target or the projectile nucleus before the complete transfer of the alpha particle. This sequential process enables the population of higher nuclear states as well as unnatural parity states [34]. Therefore, elucidating the role of two-step or multistep transfer mechanisms in the states of ^{54}Cr is also crucial.

In the present work, multiple excited states in ^{54}Cr, the heaviest stable isotope of chromium, have been populated via the ^{50}Ti(^{7}Li, t) α-transfer reaction. Since the strengths of levels populated in α-transfer reaction depend on the α-particle component of the wave function of the final state, the cluster-transfer process is expected to favor states with α + ^{50}Ti configuration. Using the light-charged particle-γ coincidence measurement, the excitation pattern has been examined, and the outcomes are reported in the form of the observed excitation energies, decay γ-ray energies, spins, integrated transfer cross sections and α-core spectroscopic factors for the excited states. In addition to the ground-state yrast band, several low-spin non-yrast states have been observed in this work. No such low-spin non-yrast states have been reported in a previous fusion evaporation study for the population of ^{54}Cr [35]. The experimental cluster-transfer cross sections for the different excited states are obtained from the respective γ-yields, and are compared with direct reaction model calculations using the code FRESCO, employing the coupled channels formalism. The results indicate the prevalence of one-step α-transfer to the ^{50}Ti target g.s. populating the low-spin states of ^{54}Cr, while for the high-spin states, a two-step transfer would facilitate larger α + core overlap than that for a one-step transfer. Since ^{54}Cr can also be produced via the complete fusion-evaporation reaction ^{50}Ti(^{7}Li,$p2n$), a comparison of the yields of the yrast states relative to the first 2^+ state has been performed for both the α-transfer and proton-induced channels, using t–γ and p–γ coincidence analyses, respectively.

The manuscript is organized as follows: Sect. 2 presents the experimental details and data analysis. Section 3 provides the results from the measurements, while Sect. 4 discusses the Coupled Reaction Channels (CRC) calculations used in this work. Section 5 provides a discussion of the results, and a summary of the experiment and findings is presented in Sect. 6.

2 Experimental details and data analysis procedure

The excited states of ^{54}Cr were populated via the α-transfer reaction ^{50}Ti(^{7}Li, t) with ^{7}Li beam energy of 20 MeV provided by the 14UD BARC-TIFR Pelletron Linac Facility at Mumbai, India. The average beam current on the target was between 4 and 5 nA. A self-supporting ^{50}Ti target (with enrichment $\approx$ 83%) having a thickness of about 1.48 mg/cm^2 was used for the present experiment. The deexciting γ-rays of residual nuclei were detected by the Indian National Gamma Array (INGA) [36,37], consisting of seventeen Compton-suppressed clover HPGe detectors, positioned at a distance of 25 cm from the target. The detectors were mounted at different angles with respect to the beam direction, with three each at 40°, 115°, 140°, and 157°, one at 65° and four at 90°. For the detection of the outgoing light-charged particles, ten CsI(Tl) detectors with dimensions of 1.5 $\times$ 1.5 $\times$ 0.3 cm^3 were mounted at a distance of 4 cm from the target position, with four centered at θ = 34°, five at 56° and one at 78°. To stop the elastically scattered particles from entering the detectors, Ta absorbers of varying thicknesses were used in front of the CsI(Tl) detectors. A Si surface barrier detector was also mounted at 6.6 cm from the target position and at an angle of 14.3^o with respect to the beamline. This monitor detector was used to measure yield of scattered beam particles for normalization.

The clover HPGe detectors have been calibrated using a mixed radioactive source of ^{133}Ba and ^{152}Eu with known γ-ray energies [38]. The typical full width at half maximum (FWHM) energy resolutions at 1.33 MeV ranged from 2.2 to 3.2 keV for the clover HPGe detectors. The absolute efficiencies of each detector at different γ-ray energy have also been determined using these sources and also reported in a previous study on the same setup [37] for higher energy. The CsI(Tl) detectors were calibrated using the triton energy spectrum of the reaction ^{12}C(^{7}Li, t)^{16}O [39] at a beam energy of 20 MeV. The signals generated due to the interaction of the γ-rays or outgoing charged particles within the detector materials were processed and recorded in list mode with a Digital Data AcQuisition (DDAQ) system [40] based on Pixie-16 modules of XIA-LLC, which can record both the energy and timing information of the incoming signal. A total of six 12-bit 100 MHz Pixie-16 modules have been used for collecting the signals from the individual CsI(Tl) and each crystal of the clover HPGe detectors. For an event in any channel of the Pixie-16 module, either a CsI(Tl) detector or a clover HPGe (in the absence of veto pulses from the BGO anti-Compton shield) generates a fast trigger having a width of 100 ns. The CsI(Tl) signals have been acquired using QDCs (charge-to-digital converters) for the identification of the different light-charged particles. The data files have been sorted by a MultipARameter time-stamped basedCOincidence Search (MARCOS) [40] code, developed at TIFR, to generate the particle-γ matrix files with two- and higher-fold coincidence events. Further, The RADWARE and ROOT software packages have been used for data analysis [41,42]. The 2D particle identification spectrum has been generated in the coincidence of CsI(Tl) with the clover HPGe detectors. All pulses from every event recorded in the CsI(Tl) detector have been preserved. To identify particles, the charges of each pulse during its rise (QDC short time = 2.5 μs) and throughout the entire pulse duration (QDC long time = 14.0 μs) were integrated. The ratio of these two integrals serves as the basis for particle identification. A 2D spectrum of QDC-short vs QDC-long for 34° CsI(Tl) detectors has been shown in Fig. 1. Proton-, triton-, and α-bands have been identified in the spectrum. The protons arise from evaporation after complete and/or incomplete fusion in the ^{7}Li + ^{50}Ti system, while the α band has contributions from the triton transfer, ^{7}Li breakup and incomplete fusion channels. The triton band originates from the no-capture ^{7}Li breakup, α-incomplete fusion and α-transfer processes. Thus, all desired information about the states populated in the recoiling ^{54}Cr nucleus by direct α cluster-transfer process can be extracted from the complementary tritons. Due to the limited energy resolution of the CsI(Tl) detectors, closely spaced states in ^{54}Cr may overlap and become indistinguishable. The experimental cross section for each state has been extracted based on its characteristic γ-decay transitions. An energy gate was applied to the particle spectrum to suppress background and isolate specific reaction channels, enabling a cleaner γ-spectrum from the clover HPGe detectors and allowing extraction of the yields for the relevant photo-peaks.

3 Experimental results

3.1 Reaction channels populating ^{54}Cr

In heavy-ion collisions, various reaction channels become energetically favorable, thereby competing with one another. Multiple channels can simultaneously contribute to the population of the same nucleus. One of the strongest is the complete-fusion evaporation reaction, which exhibits a large cross-section at above-barrier energies. In the ^{7}Li + ^{50}Ti system, nuclei such as ^{54,55}Mn, $^{53-55}$Cr are significantly populated through 3n, 2n, $p3n$, $p2n$, and pn complete fusion evaporation channels, respectively. The nucleus ^{54}Cr can also be produced through (i) α-ICF with ^{50}Ti and (ii) α cluster-transfer to ^{50}Ti. The ^{54}Cr compound nucleus in the former subsequently deexcites to $^{51-53}$Cr through xn-evaporation, as well as $^{51-53}$V via $px n$ channels, while the ^{54}Cr residual nucleus in the latter is populated in distinct excited states subject to the angular momentum transferred in the process. The various reaction pathways for the combination of the target ^{50}Ti and the weakly bound projectile ^{7}Li are illustrated

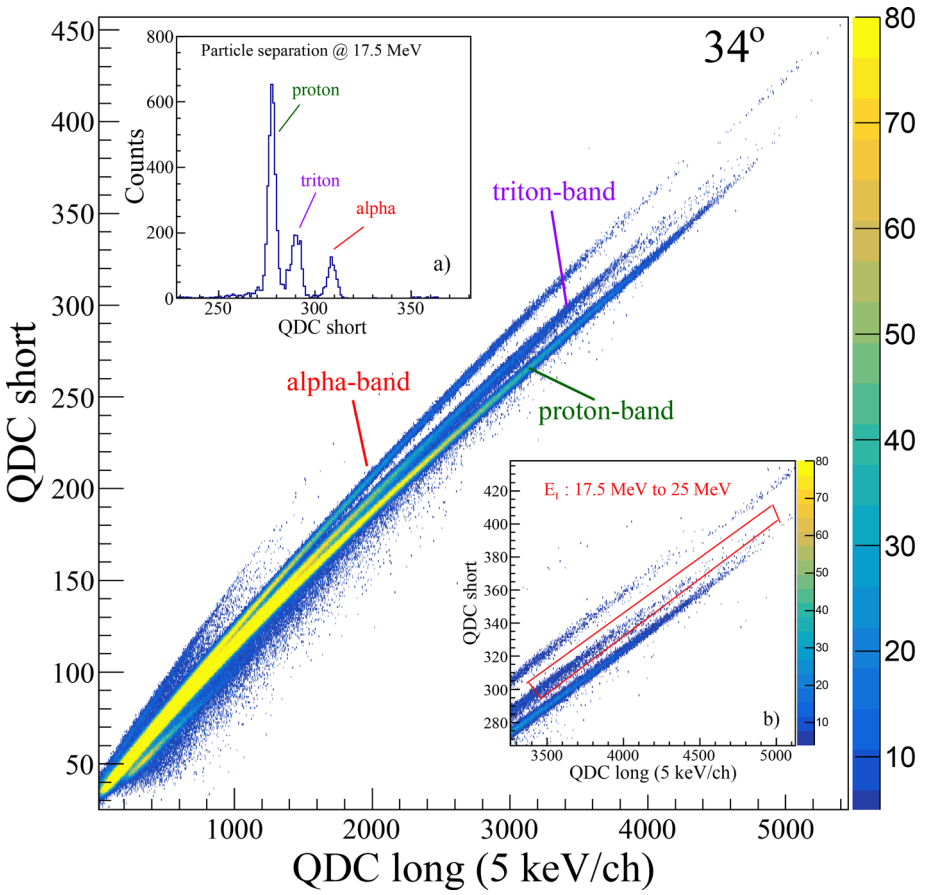

Fig. 1 Calibrated particle spectrum of a CsI (Tl) detector placed at $\theta_{lab} = 34°$ showing bands of light-charged particles—protons, tritons, and α—observed in the present measurement. The QDC short parameter is given in arbitrary units. Insets (**a**, **b**) show clear separation between the different types of particles at energy 17.5 MeV, which is chosen as the lowest triton kinetic energy, E_t, corresponding to the direct α-transfer process (see text for details)

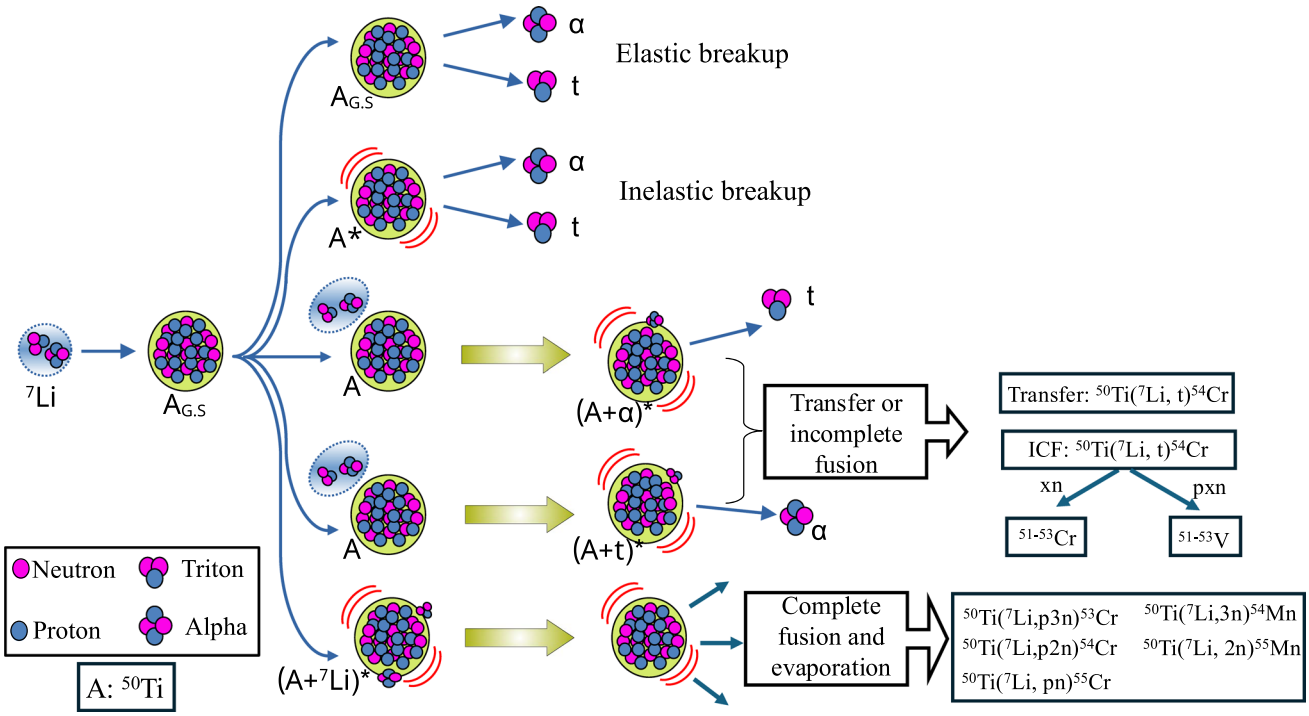

Fig. 2 Illustration of the various possible reaction pathways for the combination of the target ^{50}Ti and the weakly bound projectile ^{7}Li. Weaker reaction channels are not shown

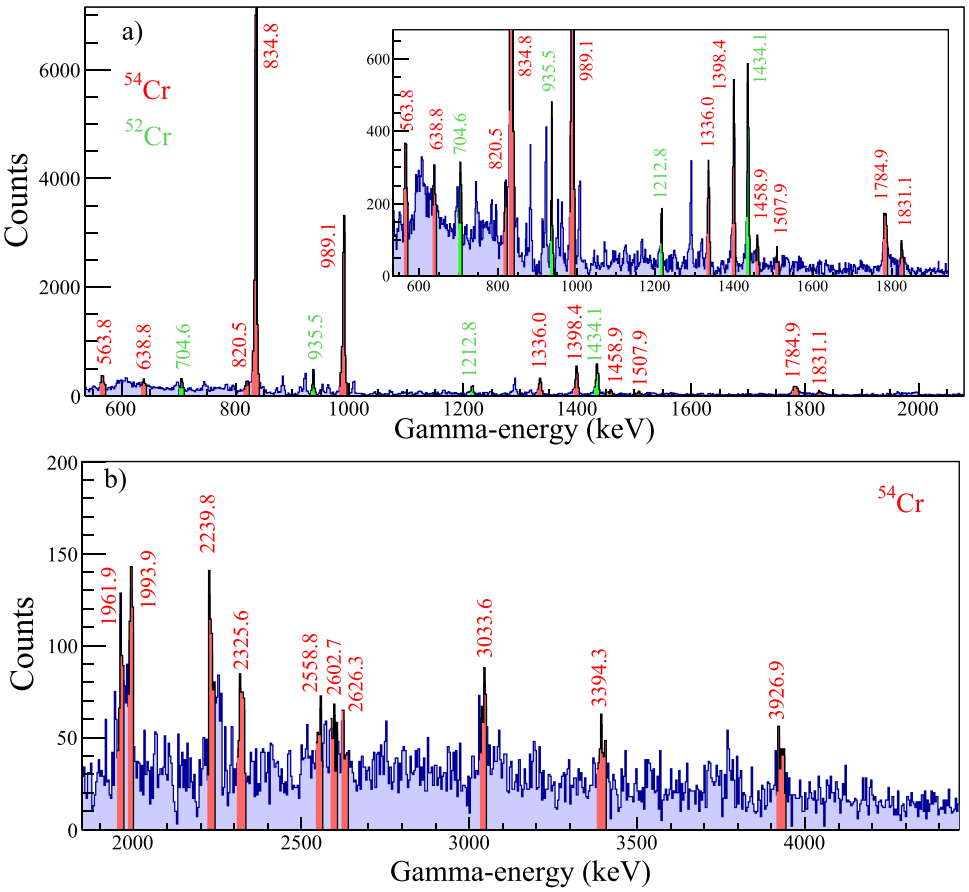

Fig. 3 The γ-ray energy spectrum with peaks in the range **a** 530 keV $< E_\gamma <$ 1.9 MeV (inset showing the same region but in a different Y scale to highlight the weaker peaks) and **b** 1.9 MeV $< E_\gamma <$ 4.5 MeV, showing decay transitions from ^{54}Cr (shaded in red) obtained in coincidence with the high energy tritons (17.5 MeV $\leq$ E$_t$ $\leq$ 25 MeV). A few transitions of ^{52}Cr are also observed (shaded in green), owing to α-transfer to ^{48}Ti present in the target material

in Fig. 2. To isolate the Cr isotopes produced by fusion evaporation, a proton band gate has been employed, allowing for the identification of the emitted γ-rays associated with each isotope. In the t-band, the tritons originating from the no-capture-projectile-breakup process as well as the α-ICF are expected to be lower in energy, peaked at around 8.5 MeV for the present bombarding energy of 20 MeV. By applying a low-energy triton gate, the γ-ray energy spectrum reveals the presence of $^{51-53}$Cr as well as $^{51-53}$V isotopes.

On the other hand, the higher-energy tritons arise from the direct α-transfer process, owing to a positive g.s. Q-value of 5.46 MeV for the transfer process. To exclude contributions from other reaction channels, tritons constrained in the kinetic energy range $\approx$ 17.5 to 25 MeV are selected to obtain the γ-ray spectrum within a 2D particle gate summed over all angles (as marked in inset (b) of Fig. 1) since these are expected to exclusively carry signatures of the α-transfer process. Here the highest triton energy, based on its outgoing angle relative to the beam direction, corresponds to the g.s. of residual ^{54}Cr nucleus. As such, levels up to an excitation of $\approx$ 5 MeV beyond the g.s. could be suitably selected at different angular positions of the particle detectors. The measured energy resolution of the CsI(Tl) detectors at $\sim$ 8 MeV is approximately 400 keV, tested using a ^{229}Th alpha source. The selected energy cut ($E_t >$ 17.5 MeV) for triton kinetic energy ensures that the 5 MeV excitation energy is well accommodated and effectively suppresses contributions from breakup tritons. In addition, since the angular coverage of the CsI(Tl) detectors ranges from 22.5° to 90°, there is negligible possibility of missing out the yields from higher excited states such as the 6^+ and 8^+ states while selecting $E_t >$ 17.5 MeV. Our calculations also account for the angular coverage of the charged particle detectors. Multiple yrast and non-yrast states of ^{54}Cr populated through α-transfer reaction have been successfully identified. The population of non-yrast states in transfer reactions are often observed to be at par with those of yrast states, unlike in in-beam fusion-evaporation reactions [43,44].

A comparison of the pattern of excited states in ^{54}Cr accessible through α-transfer as well as $p2n$ fusion evaporation can be drawn through the t-gated and p-gated γ-ray spectra as shown in Figs. 3 and 4, respectively. In a typical fusion-evaporation reaction, the compound nucleus possesses a large amount of excitation energy and angular momentum and undergoes sequential evaporation of multiple particles followed by emitting γ rays in order to reach a more stable state. The accessible decay region is bound by the yrast line that connects the lowest energy state corresponding to each angu-

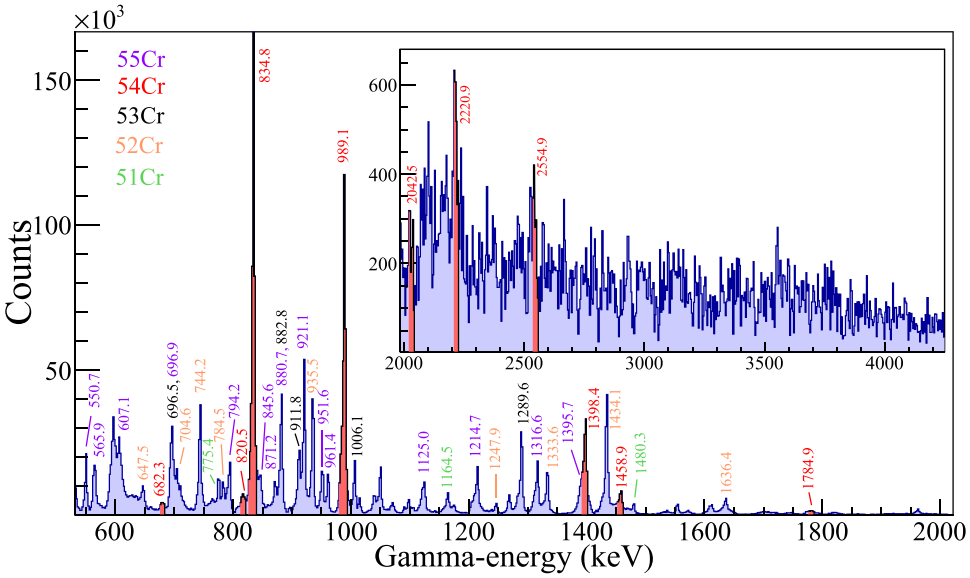

Fig. 4 The γ-ray spectrum (530 keV–2 MeV in the panel and 2 MeV–4.5 MeV in the inset) in coincidence with protons of energy $E_p \geq 8.4$ MeV (proton energy has been corrected based on the formalism mentioned in Ref. [45]), showing decay transitions from nuclei produced by pxn evaporation from the complete fusion channel. The peaks corresponding to ^{54}Cr are shaded in red color. The non-yrast states in ^{54}Cr are observed to be suppressed in the $p2n$ channel compared to that in the α-transfer channel

lar momentum. The evaporated particles carry away substantial energy, based on their separation energies, and angular momenta from the compound nucleus. As such, the yrast (and near-yrast) states become energetically favorable pathways and are often more strongly populated. On the contrary, transfer reactions, which involve the exchange of a nucleon/cluster with a specific orbital angular momentum between the projectile and the target, can lead to a higher probability of selectively populating non-yrast states, which may have specific configurations favorable for nucleon/cluster transfer. In addition to ^{54}Cr, Fig. 3 also displays transitions from ^{52}Cr, which is produced through α cluster-transfer involving ^{48}Ti present in the target. Similarly, in addition to ^{54}Cr, Fig. 4 shows peaks originating from other Cr isotopes, which may have been populated in the same reaction via the pxn channels, and/or due to the fusion of ^{7}Li with ^{48}Ti (and trace amounts of the other Ti isotopes) present in the target foil. This work reports a comprehensive investigation of the α-transfer channels exclusively.

In addition, we have compared the relative yields (with respect to the first 2^+ state) of higher-spin yrast states for the α-transfer and fusion-evaporation channels, as presented in Table 1. The relative yield of higher-spin yrast states, with respect to the first 2^+ state, decreases more sharply in transfer reactions than in fusion-evaporation reactions. This is mainly because the direct transfer of large angular momentum is less favorable for populating higher-spin levels such as 6^+ and 8^+. In contrast, fusion-evaporation reactions proceed through the formation of a compound nucleus, where the angular momentum carried by the projectile is distributed statistically, often leading to significant population of higher-spin states.

Table 1 The relative yields (with respect to the first 2^+ state) of yrast states in ^{54}Cr for both the α-transfer and proton channels

Relative yield	α-transfer channel (in %)	Proton channel (in %)
Y_{4^+}/Y_{2^+}	44.0 ± 2.5	98.7 ± 5.2
Y_{6^+}/Y_{2^+}	10.5 ± 0.7	46.6 ± 2.9
Y_{8^+}/Y_{2^+}	2.1 ± 0.3	8.4 ± 0.5

3.2 Energy states of core + α configuration

The t-gated γ-ray spectrum (17.5 MeV $\leq E_t \leq$ 25 MeV) obtained after random and background subtraction has been presented in Fig. 3a, b. The populated states in the yrast band of ^{54}Cr could be observed (shaded in red), ranging from 2^+ to $(8)^+$ (of excitation energies 834.8-, 1823.9-, 3222.3-, and 4681.2 keV). The negative parity band exhibits the observation of $(1^-, 2^-)$ and 3^- states at energies of 3393.3- and 4127.6 keV, respectively. Additionally, several low-lying non-yrast states of spins to 0^+, 2^+, and 4^+ could be populated and observed. Specifically, transitions at energies of 563.8-, 638.8-, 820.5-, 834.8-, 989.1-, 1336.0-, 1398.4-, 1458.9-, 1507.9-, 1784.9-, 1831.1-, 1961.9-, 1993.9-, 2239.8-, 2325.6-, 2558.8-, 2602.7-, 2626.3-, 3033.6-, 3394.3-, and 3926.9 keV could be identified in this study. While these transitions had been previously observed in other measurements [38,46], this experiment specifically focuses on transitions associated with the decay of α-cluster states. As such, the transfer reaction reveals strong J selectivity in the relative yields. For each observed γ-transition of interest between a pair of levels J_i and J_f, the corresponding emission cross section for decay of level J_i has been extracted using the relation,

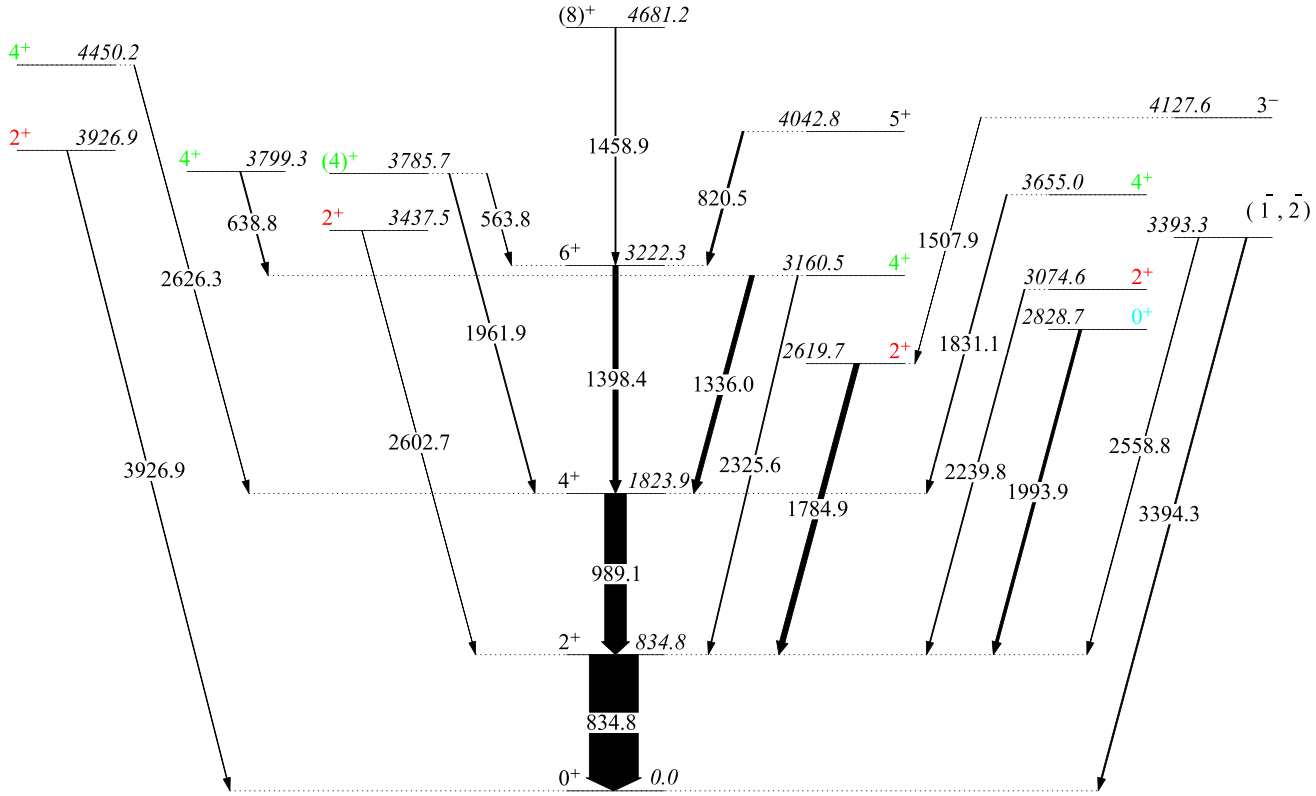

Fig. 5 Excited levels of ^{54}Cr (α + ^{50}Ti) measured in coincidence with the complementary t particles. The spins and parities are adopted from Ref. [46]. The observed non-yrast states are marked in color

$$\sigma_\gamma(J_i) = \frac{Y_\gamma(J_i)}{Y_M}\frac{d\Omega_M}{\epsilon_\gamma}\sigma_M, \tag{1}$$

where $Y_\gamma(J_i)$ and Y_M represent the yield of the γ-transition (after correction for internal conversion) and the monitor respectively, $d\Omega_M$ represents the solid angle subtended by the monitor detector, ϵ_γ is the absolute photopeak efficiency of the γ-transition, and σ_M is the Rutherford scattering cross-section (at $\theta_M = 14.3°$ w.r.t the beam direction) at the same beam energy.

The excited energy level of ^{54}Cr, E_i, can be populated either directly from the α-transfer reaction or indirectly through γ-ray decay from higher energy levels E_j (where $E_j > E_i$), called feeding or indirect population. The direct population of a nuclear level E_i is calculated by subtracting the feeding contributions from higher-lying levels E_j:

$$Y_{direct}(E_i) = Y_\gamma(E_i) - \sum Y_\gamma(E_j \rightarrow E_i) \tag{2}$$

Where, $Y_{\text{direct}}(E_i)$ and $Y_\gamma(E_i)$ are the yields of the direct population of level E_i and the observed γ-ray emitted from the level E_i, respectively. $Y_\gamma(E_j \rightarrow E_i)$ denotes the γ-ray yield that feeds into E_i from higher energy level E_j. The feeding contributions to the measured yields after the efficiency correction of the different γ-lines, as shown in Fig. 5, have been subtracted prior to the determination of the emission cross sections.

During γ emission, a level J_i decays to a level J_f. However, during α transfer, the level J_i is directly populated. To determine the population cross section for each state J_i, the emission cross section has been multiplied by the factor $(2J_i + 1)/(2J_f + 1)$. For states decaying by more than one γ-transition, the net experimental cross-section is obtained by summing over each individual emission cross-section, weighted by the corresponding branching as available in literature [38,46].

3.3 Spectroscopic factors

One of the principal highlights of this study is the determination of the α+core spectroscopic factors for both the yrast and non-yrast states in ^{54}Cr. In the context of α-transfer, the spectroscopic factor indicates the probability of an α particle transferred as a single entity in one step to the target nucleus, populating excited states of the residual nucleus. The structure of excited states of the composite nucleus is predominantly given by a bound core with the transferred α-particle populating any of its available higher levels, by coupling to the core ground state or excited state. The α particle

Table 2 Level energies E_x and measured integrated cross-sections σ_{expt} for the population of the excited I) yrast and II) non-yrast states of ^{54}Cr observed in the present measurement, arranged in order of increasing excitation energies. Each energy level J_i has been identified by the associated γ transition $J_i \rightarrow J_f$, of energy E_γ. The spins J_i^π and relative orbital angular momenta ℓ_{tr} between the α-particle and ^{50}Ti core incorporated in FRESCO calculations are also indicated. The corresponding α-core spectroscopic factor ($S_{\ell j}$) has been obtained by normalizing the calculated cross sections with the measured values. The $S_{\ell j}$ value for the population of the ground state of ^{54}Cr is taken as 0.16, as reported in Ref. [30]

Energy level E_x(keV)	[a]Spin J_i^π	[b]Observed E_γ (keV)	$J_i \rightarrow J_f$	[c]Population cross-section, σ_{expt} (μ b)	ℓ_{tr} ($\hbar$)	Spectroscopic factor ($S_{\ell j}$)	
						This work	In literature
(I) Yrast states							
834.8	2^+	834.8(1)	$2^+ \rightarrow 0^+$	19.95(159)	2	0.1118(89)	0.0752 [30]
1823.9	4^+	989.1(1)	$4^+ \rightarrow 2^+$	4.99(41)	4	0.0296(24)	0.0224 [30]
3222.3	6^+	1398.4(2)	$6^+ \rightarrow 4^+$	0.65(06)	6	0.0018(2)	–
〃	〃	〃	〃	〃	[d]2,4	0.0871(75)	-
3393.3	$(1^-, 2^-)$	2558.8(8), 3394.3(14)	$(1^-, 2^-) \rightarrow 2^+, 0^+$	0.81(20)	[e]1	0.0460(87)	–
4042.8	5^+	820.5(2)	$5^+ \rightarrow 6^+$	0.50(07)	[d]2,4	0.8019(882)	–
4127.6	3^-	1507.9(4)	$3^- \rightarrow 2^+$	0.10(03)	3	0.0006(2)	–
4681.2	$(8)^+$	1458.9(5)	$(8)^+ \rightarrow 6^+$	0.40(07)	8	0.0009(1)	–
〃	〃	〃	〃	〃	[d]4,6	0.0319(47)	–
(II) Non-yrast states							
2619.7	2^+	1784.9(4)	$2^+ \rightarrow 2^+$	1.30(16)	2	0.0015(2)	–
2828.7	0^+	1993.9(9)	$0^+ \rightarrow 2^+$	0.17(04)	0	0.0021(4)	–
3074.6	2^+	2239.8(9)	$2^+ \rightarrow 2^+$	0.28(08)	2	0.0003(1)	–
3160.5	4^+	1336.0(1), 2325.6(7)	$4^+ \rightarrow 4^+, 2^+$	1.16(11)	4	0.0065(6)	–
3437.5	2^+	2602.7(9)	$2^+ \rightarrow 2^+$	0.10(05)	2	0.00010(4)	–
3655.0	4^+	1831.1(3)	$4^+ \rightarrow 4^+$	0.31(08)	4	0.0014(3)	–
3785.7	$(4)^+$	563.8(3), 1961.9(7)	$4^+ \rightarrow 6^+, 4^+$	0.24(03)	4	0.0019(2)	–
3799.3	4^+	638.8(7)	$4^+ \rightarrow 4^+$	0.26(05)	4	0.0024(4)	–
3870.4	–	3033.6(12)	–	–	–	–	
3926.9	2^+	3926.9(17)	$2^+ \rightarrow 0^+$	0.98(30)	2	0.0009(2)	–
4450.2	4^+	2626.3(12)	$4^+ \rightarrow 4^+$	0.12(05)	4	0.0004(1)	–

[a] Spin values as per Ref. [46]
[b] γ-transitions identified from random- and background-subtracted t-gated spectra
[c] $\sigma_{\text{expt}} = \sigma_\gamma(J_i) \times (2J_i + 1)/(2J_f + 1)$ gives the cross section for population of state J_i integrated over the measured angular range
[d] The core nucleus is considered to have been in an excited state prior to the α-transfer i.e., two-step process
[e] The experimental cross-section has been compared with calculations assuming the spin of the excited state as 1^-

wave function and the ^{50}Ti target nucleus wave function need to overlap to allow the transfer process to populate excited states in the residual nucleus. A strong overlap indicates a higher probability of finding the transferred α particle in the specific state. Experimental measurements of the spectroscopic factor in α-transfer reactions provide valuable information about the structure of nuclei and the occupancy of excited states. In the present reaction, this overlap probability $S_{\text{expt}} = |\langle ^{54}\text{Cr} \,|\alpha + ^{50}\text{Ti}\rangle|^2$ is obtained by comparing the measured cross-sections with standard model calculations, often in the DWBA limit.

$$S_{\text{expt}} = \frac{\sigma_{\text{expt}}}{\sigma_{\text{DWBA}}} \tag{3}$$

The excited states of ^{54}Cr could not be individually resolved in the particle energy spectrum since the energy resolution of the CsI(Tl) detectors is approximately 350–400 keV. To overcome this, high-resolution HPGe detectors are used to identify and separate the excited states by detecting the associated γ rays. The ratio of the measured cross-sections (σ_{expt}) for individual states and the calculated the integrated cross-section (σ_{DWBA}) within the angular coverage of the particle detectors provide the corresponding spectroscopic factors.

4 FRESCO Calculations

To draw conclusions about the strength of the $\alpha + ^{50}$Ti core overlap in each observed state of ^{54}Cr, i.e. the corresponding spectroscopic factor, extensive calculations have been carried out using the code FRESCO [47]. The total potential for the interacting system is defined as:

$$U(r) = V_c(r, R_c) - \frac{V_0}{1+\exp(\frac{r-R_0}{a_0})} - \frac{iW_0}{1+\exp(\frac{r-R_w}{a_w})} \quad (4)$$

Here, $V_c(r, R_c)$ is the Coulomb potential due to a uniformly charged sphere, and V_0 and W_0 are the depths of the real and imaginary components of the nuclear optical potential, with diffuseness a_0 and a_w, respectively. The corresponding radii are defined as $R_{c/0/w} = r_{c/0/w}(A_P^{1/3} + A_T^{1/3})$, with r_c taken to be 1.2 fm and A_P and A_T are the projectile and target masses, respectively. Optical potential parameters have been obtained from a global systematic parameterization for ^{7}Li projectile [48]. For completeness of the calculations, the bound state of ^{7}Li at 478 keV, as well as the 2_1^+ and 4_1^+ levels of ^{50}Ti are also coupled, using B(E2) values reported in Refs.[38,49,50]. For exact coupling in the model space, the target excited states were taken as vibrational excitations, while a rotational model picture has been used for the projectile excitation. For a weakly bound nucleus such as ^{7}Li, the coupling of its breakup channels along with bound excited states is often incorporated into the model space of calculations. However, the simultaneous coupling of inelastic states, α-transfer channels as well as projectile continuum channels is often computationally demanding. So, the current calculations include only the bound excited states and α-transfer channels with no consideration given to the breakup channel. The volume absorptive imaginary potential, i.e; $W(r)$, accounts for the flux lost from the elastic channel to nonelastic direct channels excluded from the calculations, which comprise of breakup, one-nucleon/multi-nucleon transfers, and incomplete fusion. Furthermore, this potential accommodates the compound reaction occurring in the entrance channel.

For the α-transfer exit channels, the real part of the $t + ^{54}$Cr phenomenological potential, as well as the spin-orbit potential, are obtained using Ref [51]. A short-ranged Woods-Saxon imaginary potential, given by W_0 = 10.00 MeV, r_w = 1.00 fm, and a_w = 0.40 fm, is used to account for the absorption of flux from the exit channels. The α-t binding potential for the g.s. of ^{7}Li is taken to be of a Gaussian form as mentioned in Ref. [52]. The amplitude for the overlap $\langle ^7\text{Li}|\alpha + t\rangle$ is taken as 1.01 [53]. The binding potential of the transferred α-particle to the ^{50}Ti core is chosen to be of Woods-Saxon volume form, where the depth is automatically adjusted to achieve the required binding energies of the particle-core composite system in each excited state of ^{54}Cr. The coupling scheme used for the fresco calculations is graphically shown in Fig. 6. The system of coupled equations is solved in the DWBA limit for the α-transfer process, to explain the experimental cross sections and further determine the relevant structural parameters for each excited state. The elastic scattering, projectile inelastic scattering, and target inelastic scattering channels are solved exactly, while the weaker transfer channels are calculated as a first-order perturbation.

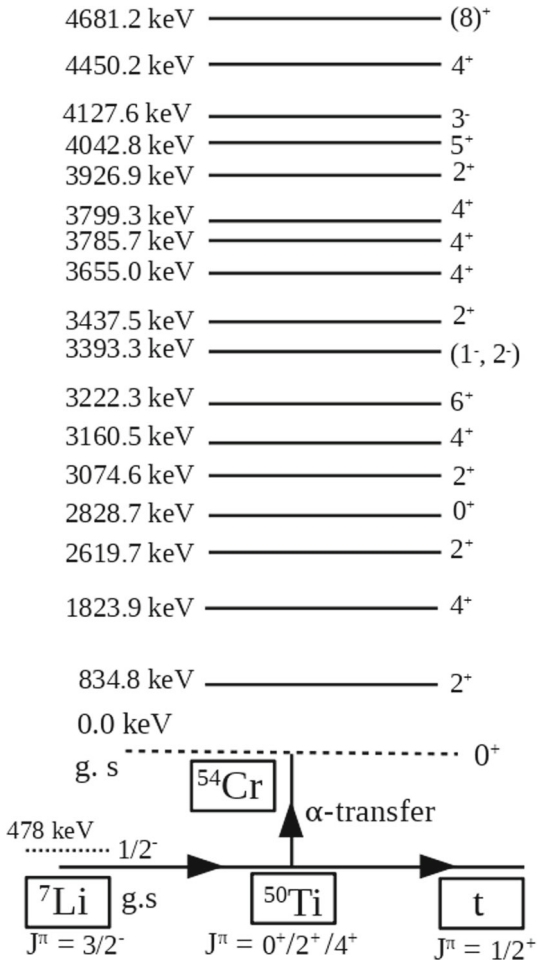

Fig. 6 Coupling scheme used for the FRESCO calculations. The projectile and target excited states are solved exactly while the transfer channels are solved in first-order perturbation. The transfer channels are those which have been exclusively identified in the present work by means of t-γ coincidence

For achieving convergence of the calculations in the current angular range of interest, integrating to 50 fm in steps of 0.25 fm and using 60 partial waves were found to be adequate. Fixing the quantum numbers of the final states of the residual nucleus and specifying the spectroscopic factors allows comparisons between calculations and data. Extracted spectroscopic factors are determined through the normalization to the experimentally measured angle-integrated cross-section. In cases where these structural parameters were unavailable, new values have been assigned to obtain optimum agreement with the experimental data (see Table 2). Since the present measurement does not provide the spectroscopic information about the g.s. of the ^{54}Cr nucleus, the corresponding spectroscopic factor was fixed as 0.16, as reported in Ref. [30] for completeness of the calculations.

While calculating the spectroscopic factors (SFs), an additional model-dependent systematic uncertainty needs to be

Table 3 The two optical model potentials used with their parameters

Parameters	Potential-1 (Ref. [48])	Potential-2 (Ref. [54])
V_0 (MeV)	114.2000	40.2000
r_0 (fm)	0.8460	1.1500
a_0 (fm)	0.8530	0.5530
W_0 (MeV)	25.4100	15.4100
r_w (fm)	1.1440	1.1800
a_w (fm)	0.8090	0.5090

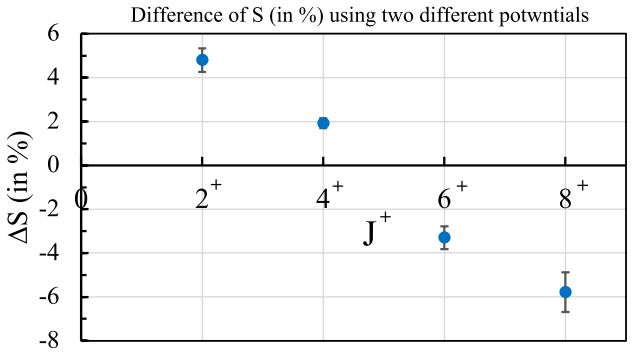

Fig. 7 The percentage difference between the spectroscopic factors (S) obtained using the two sets of optical model parameters for potential-1 [48] and potential-2 [54]

considered due to the choice of optical model parameters. To obtain this effect, we selected two distinct sets of optical model potentials parameters (Table 3) from previous studies.

The integrated cross sections were then calculated using these two sets of optical potentials within the defined solid angle range. Finally, we calculated the percentage difference in the spectroscopic factors (S) obtained using the two sets of optical model parameters. The variation in S for the yrast states between these two potential sets is presented in Fig. 7. The observed differences are within 7%, which suggests less sensitivity of the integrated cross sections on the choice of the optical potential parameters within the angular range of interest.

5 Discussion

Proton-, triton-, and α-bands have been identified in the 2D particle spectrum (Fig. 1), and the corresponding favorable reaction channels are illustrated in Fig. 2. A deuteron band is also expected to arise from either (a) the one-neutron transfer-induced breakup of ^{6}Li into $\alpha + d$, or (b) the direct breakup of ^{7}Li into $^6\text{Li} + n$, followed by the subsequent dissociation of ^{6}Li into $\alpha + d$. However, based on kinematics, the peak kinetic energy of the deuteron is expected to be less than 6 MeV for both processes (a) and (b). This spectrum is expected to merge with the low-energy proton and triton bands and not separated in the particle spectrum. In the limit of energy resolution of the CsI(Tl) detectors, closely-spaced states in ^{54}Cr can become mixed. The experimental cross-section for each state has been determined on the basis of the decay γ-transitions from the same.

The γ-ray spectrum of the clover HPGe detectors was cleaned by applying energy gates to the particle spectrum to extract the yields of the corresponding photo-peaks of interest. The α-transfer t-gated and p-gated γ-ray spectra (Figs. 3 and 4) show well-resolved ^{54}Cr transitions. In addition to ^{54}Cr, Fig. 3 also displays few transitions from ^{52}Cr, which is produced via α cluster-transfer involving ^{48}Ti present in the target foil.

The relative yields (with respect to the first 2^+ state) of higher-spin yrast states (6^+ and 8^+) decreases more sharply in transfer reactions than in fusion-evaporation reactions (Table 1). This is primarily due to the fact that direct transfer reactions are less effective at populating those higher-spin states because the transfer of large angular momentum is less favorable. In contrast, fusion-evaporation reactions involve the formation of a compound nucleus, where the projectile's angular momentum is statistically distributed among available states, often resulting in a substantial population of higher-spin levels.

The α-core spectroscopic factors for the yrast 2^+ and 4^+ states obtained in the present work reasonably agree with those available in the literature for ^{54}Cr [30]. However, the α-core spectroscopic factors for five additional yrast states and eleven non-yrast states have been newly measured in this work, as presented in Table 2. For few excited states-specifically at 4127.6-, 4681.2-, 3074.6-, 3437.5-, 3926.9-, and 4450.2 keV-the α-core spectroscopic factors are quite small (on the order of 10^{-4}), indicating that these states are weakly populated via the α-transfer from ground state of ^{50}Ti. This suggests a minimal contribution from an α+core configuration in their structure. The uncertainties in the extracted spectroscopic factors reach up to 30% for a few states (Table 2), primarily due to the uncertainty of intensity of the observed gamma rays from weakly populated transitions. The values of extracted spectroscopic factor for the 2^+ and 4^+ states are of the same order as those reported for ^{32}S [14] and ^{46,48}Ti [30]. Comparing the results with those obtained for ^{40}Ca [55] and ^{44}Ti [30], one observes that while the 2^+ state of ^{54}Cr has a spectroscopic factor in a similar range, the value for the 4^+ state is lower. In a previous study [56], the α-transfer cross section for the ground state and the first 2^+ excited state of ^{54}Cr was measured via the ^{50}Ti(^{16}O,^{12}C)^{54}Cr reaction at a beam energy of 48 MeV, yielding a cross section of 7.8 μb/sr. The data were recorded at two laboratory angles between 35° and 50°. In contrast, our experiment, performed using a different projectile-target (^{7}Li on ^{50}Ti) combination at a laboratory energy of 20 MeV and covering a wider angular range from 22.5° to 90°, mea-

sured the cross section for the first 2^+ state to be 19.95(159) μb/sr.

The coupling scheme showing α-transfer from the states of ^{50}Ti is illustrated in Fig. 6. A two-step transfer process is also considered for a few excited states (5^+, 6^+, and 8^+) of ^{54}Cr where the ^{50}Ti core is in its excited state (2_1^+ or 4_1^+) prior to the α transfer. This would allow for multiple lower values of transferred relative orbital angular momentum, $\ell_{\rm tr}$, to participate in the population of that specific state in the composite nucleus. To populate higher-spin states such as 8^+ and 6^+ from the ground state of ^{50}Ti, high orbital angular momentum transfers ($\ell = 8\hbar$ and $6\hbar$, respectively) are required. However, if the alpha transfer occurs from an excited state of ^{50}Ti (e.g., from the 2^+ or 4^+ state), lower ℓ values can effectively populate these higher-spin states. Hence, the corresponding spectroscopic factors for these higher-spin states are found to be larger than those obtained from a single-step transfer process, indicating an enhanced contribution from the two-step transfer mechanism in facilitating an α + core configuration in these states. However, for the population of the yrast 2^+ and 4^+ states, α-transfer is observed to be a predominantly single-step process.

The population of the unnatural-parity state, 5^+, is not possible through a single-step α-transfer process. Therefore, a two-step transfer mechanism was considered to account for its population and to explain the observed yield. The 5^+ state can be explained by considering α-transfer to the excited states, 2^+ or 4^+ of ^{50}Ti, where the angular momentum transfer ($\ell = 4\hbar$ or $2\hbar$) is lower and can effectively populate 5^+ state. The large spectroscopic factor of this state indicates a strong overlap between the α particle and the excited ^{50}Ti core, facilitating the formation of the unnatural-parity 5^+ state.

In contrast, for the 1^- natural-parity state, one-step transfer process was used. The spin-parity assignments were adopted from NNDC, where the 3393.3 keV state has two tentative assignments: 1^- as well as 2^-. For completeness, both possibilities are listed in Table 2; however, the 1^- assignment was assumed in our calculations, as noted in footnote (e).

Souza et al. (Ref. [32]) suggest that ^{46}Cr and ^{54}Cr are the most favorable even-even Cr isotopes for the α + core configuration. While we have investigated ^{54}Cr through an α-transfer reaction in this work, the unavailability of a stable projectile-target combination to populate ^{46}Cr limits the exploration of α + core structures in the ^{46}Cr nucleus.

In addition, a model-dependent systematic uncertainty is anticipated due to the choice of optical model parameters. To address this, we have considered two distinct sets of optical model potential parameters, as listed in Table 3, based on values reported in the literature. The percentage difference in the spectroscopic factors (S) was calculated using these two sets of optical model parameters for the yrast states of ^{54}Cr. The observed variation is within 7% (as shown in Fig. 7), indicating that the integrated cross-sections are less sensitive to the choice between these two optical potential parameter sets within the angular range of interest.

6 Conclusion

This study is focused on investigating low-lying states in ^{54}Cr through particle-γ coincidence measurement using the transfer reaction ^{50}Ti(^{7}Li, t). Appropriate energy selections have been applied to the t-band to disentangle the set of states populated with the α+^{50}Ti core configuration while eliminating contributions from other reactions channels. Multiple yrast states in ^{54}Cr could be suitably excited, along with several low-lying non-yrast states that are typically difficult to populate via heavy-ion fusion evaporation reactions. The relative yields of the yrast states, with respect to the first 2^+ state, have been compared for both the proton and α-transfer channels. The α-spectroscopic factor has been extracted for each state of ^{54}Cr, and the values for the 2^+ and 4^+ excited states at 834.8 keV and 1823.9 keV, respectively, are in reasonable agreement with those reported in Ref. [30]. The α+core overlaps for the yrast 2^+ and 4^+ states are found to dominate over those for the yrast 6^+ and $(8)^+$ states when the α-particle is considered to be transferred in a single-step to the core ground state. For yrast states with $J \geq 5$ in ^{54}Cr, a two-step transfer approach has also been invoked to understand the α + core configuration. However, this needs further investigation using particle detectors with better energy resolution to provide a clear identification between α-transfer involving the target g.s. compared to that involving the target excited state. The extracted α-spectroscopic factors for the 2^+, and 4^+ states have also been compared with those obtained for nuclei where the phenomenon of α-clustering has been well explored, such as ^{32}S, ^{40}Ca and ^{44,46,48}Ti. In this view, further investigations are required for the ^{54}Cr nucleus to draw firm conclusions about α-cluster structure with a more advanced setup consisting of high-resolution Si detectors with larger solid-angle coverage replacing the present CsI(Tl) detectors. Simultaneous measurements of γ-rays along with the angular distribution of triton for the α-transfer cross sections would contribute to our understanding of α+core structures in ^{54}Cr.

Acknowledgements The authors acknowledge the TIFR-BARC Pelletron Linac Facility for providing a stable beam, as well as the Center for Accelerator Target Science at Argonne National Laboratory for providing the ^{50}Ti target used in this experiment. The help and cooperation from R. Donthi for setting up the experimental apparatus are acknowledged. This work is supported by the Department of Atomic Energy, Government of India (Project Identification Code: 12-R&D-TFR-5.02-0200), the Department of Science and Technology, Government of India (Grant no. IR/S2/PF-03/2003-II), and by the U. S. National Science Foundation (Grant no. PHY-2011890). The authors would also like to thank Prof. A. Navin and Prof. R. Chatterjee for useful discussion.

Funding Open access funding provided by Department of Atomic Energy.

Data Availability Statement Data will be made available on reasonable request. [Author's comment: All the relevant data supporting the findings of the present study are given in the paper. Additional data can be provided by the corresponding author on reasonable request.]

Code Availability Statement Code/software will be made available on reasonable request. [Authors' comment: The software used in this work is available from the corresponding author on reasonable request.]

References

1. P.E. Hodgson, E. Běták, Cluster emission, transfer and capture in nuclear reactions. Phys. Rep. **374**, 1–89 (2003)
2. G.S. Li, J.G. Wang, J. Lubian, H.O. Soler, Y.D. Fang, M.L. Liu, N.T. Zhang, X.H. Zhou, Y.H. Zhang, B.S. Gao, Y.H. Qiang, S. Guo, S.C. Wang, K.L. Wang, K.K. Zheng, R. Li, Y. Zheng, Fusion reactions in the ^{9}Be+^{197}Au system above the Coulomb barrier. Phys. Rev. C **100**, 054601 (2019)
3. R.J. Woolliscroft, N.M. Clarke, B.R. Fulton, R.L. Cowin, M. Dasgupta, D.J. Hinde, C.R. Morton, A.C. Berriman, Breakup and transfer processes in the ^{9}Be+^{208}Pb reaction. Phys. Rev. C **68**, 014611 (2003)
4. R. Rafiei, R. du Rietz, D.H. Luong, D.J. Hinde, M. Dasgupta, M. Evers, A. Diaz-Torres, Mechanisms and systematics of breakup in reactions of ^{9}Be at near-barrier energies. Phys. Rev. C **81**, 024601 (2010)
5. S.K. Pandit, A. Shrivastava, K. Mahata, N. Keeley, V.V. Parkar, R. Palit, P.C. Rout, K. Ramachandran, A. Kumar, S. Bhattacharyya, V. Nanal, S. Biswas, S. Saha, J. Sethi, P. Singh, S. Kailas, Unraveling the reaction mechanism for large alpha production and incomplete fusion in reactions involving weakly bound stable nuclei. Phys. Lett. B **820**, 136570 (2021)
6. D.R. Haenni, T.T. Sugihara, R.P. Schmitt, G. Mouchaty, U. Garg, In-beam spectroscopy of neutron-rich nuclei: New application of massive-transfer reactions. Phys. Rev. C **25**, 1699 (1982)
7. G.D. Dracoulis, A.P. Byrne, T. Kibédi, T.R. McGoram, S.M. Mullins, Incomplete fusion as a spectroscopic tool. J. Phys. G: Nucl. Part. Phys. **23**, 1191–1202 (1997)
8. S.M. Mullins, G.D. Dracoulis, A.P. Byrne, T.R. McGoram, S. Bayer, R.A. Bark, R.T. Newman, W.A. Seale, F.G. Kondev, Rotational and intrinsic states above the $K^{\pi} = 25/2^{-}$, $T_{1/2} = 25$ day isomer in ^{179}Hf. Phys. Rev. C **61**, 044315 (2000)
9. R.M. Clark, L.W. Phair, M. Descovich, M. Cromaz, M.A. Deleplanque, P. Fallon, I.Y. Lee, A.O. Macchiavelli, M.A. McMahan, L.G. Moretto, E. Rodriguez-Vieitez, S. Sinha, F.S. Stephens, D. Ward, M. Wiedeking, L.A. Bernstein, J.T. Harke, J.A. Church, Population of nuclei via ^{7}Li-induced binary reactions. Phys. Rev. C **72**, 054605 (2005)
10. B. Andrea Jungclaus, A. Binder, T. Dietrich, H. Härtlein, Ch. Bauer, D. Gund, D. Pansegrau, D. Schwalm, E. Bazzacco, S. Farnea, C. Lunardi, C. Rossi-Alvarez, G. de Ur, A. Angelis, D.R. Gadea, X.R. Napoli, Zhou, Y. Sun, Excited bands and signature dependent electromagnetic decay properties in neutron-rich ^{159,161,163}Dy. Phys. Rev. C **67**, 034302 (2003)
11. D.S. Judson, A.M. Bruce, T. Kibédi, G.D. Dracoulis, A.P. Byrne, G.J. Lane, K.H. Maier, C.-B. Moon, P. Nieminen, J.N. Orce, M.J. Taylor, Structure of the isomeric states in ^{123,125}Sb. Phys. Rev. C **76**, 054306 (2007)
12. S. Bottoni, S. Leoni, B. Fornal, R. Raabe, K. Rusek, G. Benzoni, A. Bracco, F.C.L. Crespi, A.I. Morales, P. Bednarczyk, N. Cieplicka-Oryńczak, W. Królas, A. Maj, B. Szpak, M. Callens, J. Bouma, J. Elseviers, H. De Witte, F. Flavigny, R. Orlandi, P. Reiter, M. Seidlitz, N. Warr, B. Siebeck, S. Hellgartner, D. Mücher, J. Pakarinen, M. Vermeulen, C. Bauer, G. Georgiev, R.V.F. Janssens, D. Balabanski, M. Sferrazza, M. Kowalska, E. Rapisarda, D. Voulot, M. Lozano Benito, F. Wenander, Cluster-transfer reactions with radioactive beams: a spectroscopic tool for neutron-rich nuclei. Phys. Rev. C **92**, 024322 (2015)
13. M.E. Cobern, D.J. Pisano, P.D. Parker, Alpha-transfer reactions in light nuclei. III. (^{7}Li, t) stripping reaction. Phys. Rev. C **14**, 491 (1976)
14. T. Madhusoodhanan, R. Samit Mandal, M. Raja. Shyam, M.T. Rao, N.G. Lagare, A. Puttaswamy, D.K. Mandal, Avasthi, S. K. Datta, Study of α-transfer reaction ^{28}Si(^{7}Li;t)^{32}S. J. Phys. G Nucl. Part. Phys. **25**, 1897–1907 (1999)
15. F.D. Becchetti, J. Jänecke, C.E. Thorn, Nucl. Phys. A **305**, 313 (1978)
16. F.D. Becchetti, E.R. Flynn, D.L. Hanson, J.W. Sunier, ^{12}C(^{7}Li, t)^{16}O and stellar helium fusion. Nucl. Phys. A **305**, 293 (1978)
17. B. Apagyi, T. Vertse, Configuration mixing effect in the ^{12}C(^{6}Li, d)^{16}O* α-transfer reaction. Phys. Rev. C **21**, 779 (1980)
18. T. Yamaya, M. Saito, M. Fujiwara, T. Itahashi, K. Katori, T. Suehiro, S. Kato, S. Hatori, S. Ohkubo, Alpha-cluster bands in ^{40}Ca observed via the (^{6}Li, d) reaction. Phys. Lett. B **306**, 1 (1993)
19. W. Oelert, G.P.A. Berg, A. Djaloeis, C. Mayer-Böricke, P. Turek, (d, ^{6}Li)$alpha - transferreactionon^{32}$S and ^{34}S at $E_d = 80$ MeV. Phys. Rev. C **28**, 73 (1983)
20. F. Pühlhofer, H.G. Ritter, R. Bock, G. Brommundt, H. Schmidt, K. Bethge, Investigation of the reaction ^{12}C(^{7}Li, t)^{16}O. Nucl. Phys. A **147**, 258 (1970)
21. T. Matsuse, M. Kamimura, Y. Fukushima, Study of the alpha-clustering structure of ^{20}Ne based on the resonating group method for ^{16}O + α. Progress Theor. Phys. **53**(3) (1975)
22. A.C. Dreyfuss, K.D. Launey, J.E. Escher, G.H. Sargsyan, R.B. Baker, T. Dytrych, J.P. Draayer, Clustering and α-capture reaction rate from ab initio symmetry-adapted descriptions of ^{20}Ne. Phys. Rev. C **102**, 044608 (2020)
23. Yoshikazu Fujiwara, Cluster-structure study of 20Ne by "(^{16}O-α)+(^{12}C - ^{8}Be)" coupled channel orthogonality condition model. III: Alpha-decay properties, electric transitions and discussion of higher excited states. Progress Theoret. Phys. **62**(1), 138–152 (1979)
24. P. Descouvemont, D. Baye, The α+^{20}Ne cluster structure of ^{24}Mg in a microscopic three-cluster model. Nucl. Phys. A **475**(2), 219–232 (1987)
25. Y. Taniguchi, Y. Kanada-En'yo, M. Kimura, Cluster structures and super deformation in ^{28}Si. Phys. Rev. C **80**, 044316 (2009)
26. T. Lönnroth, M. Norrby, V.Z. Goldberg, G.V. Rogachev, M.S. Golovkov, K.-M. Källman, M. Lattuada, S.V. Perov, S. Romano, B.B. Skorodumov, G.P. Tiourin, W.H. Trzaska, A. Tumino, A.N. Vorontsov, Highly excited alpha-cluster states in ^{32}S studied with

the thick-target inverse kinematics method. Eur. Phys. J. A **46**, 5–16 (2010)
27. W. Bauhoff, H. Schultheis, R. Schultheis, Alpha-cluster structure of ^{32}S. Phys. Rev. C **22**, 861 (1980)
28. Takashi Yamaya, Kenji Katori, Mamoru Fujiwara, Seigo Kato, Shigeo Ohkubo, Alpha-cluster study of ^{40}Ca and ^{44}Ti by the (^{6}Li, d) reaction. Progress Theor. Phys. Suppl. **132**, 73 (1998)
29. T. Sakuda, S. Ohkubo, Cluster structure and collective behavior of the nucleus ^{48}Cr. Nucl. Phys. A **712**(1–2), 59–71 (2002)
30. H.W. Fulbright, C.L. Bennett, R.A. Lindgren, R.G. Markham, S.C. McGuire, G.C. Morrison, U. Strohbusch, J. Töke, Four-nucleon transfer via the (^{6}Li, d) reaction. Nucl. Phys. A **284**(329), (1977)
31. U. Strohbusch, C.L. Fink, B. Zeidman, R.G. Markham, H.W. Fulbright, R.N. Horoshko, (^{6}Li, d)$reaction on^{40}$Ca. Phys. Rev. C **9**, 965 (1974)
32. M.A. Souza, H. Miyake, Search for α + core states in even-even Cr isotopes. Eur. Phys. J. A **53**, 146 (2017)
33. I.J. Thompson, Coupled reaction channels calculation in nuclear physics. Comput. Phys. Rep. **7**, 167–212 (1988)
34. W.D. Weintraub, N. Keeley, K.W. Kemper, K. Kravvaris, F. Maréchal, D. Robson, B.T. Roeder, K. Rusek, A. Volya, Coupled reaction channels calculation in nuclear physics. Phys. Rev. C **100**, 024604 (2019)
35. M. Devlin, D.R. LaFosse, F. Lerma, D. Rudolph, D.G. Sarantites, P.G. Thirolf, Yrast spectroscopy of ^{54}Cr. Phys. Rev. C **61**, 017301 (1999)
36. R. Palit, Recent results from digital INGA at BARC–TIFR Pelletron Linac Facility and future plans. Pramana **83**, 719 (2014)
37. S. Saha, R. Palit, J. Sethi, S. Biswas, P. Singh, Geant4 simulation study of Indian National Gamma Array at TIFR. JINST **11**, P03030 (2016)
38. NNDC Homepage, https://www.nndc.bnl.gov
39. W.D. Weintraub, N. Keeley, K.W. Kemper, K. Kravvaris, F. Maréchal, D. Robson, B.T. Roeder, K. Rusek, A. Volya, Analyzing powers and the role of multistep processes in the ^{12}C(^{7}Li, t)^{16}O reaction. Phys. Rev. C **100**, 024604 (2019)
40. R. Palit, S. Saha, J. Sethi, T. Trivedi, S. Sharma, B.S. Naidu, S. Jadhav, R. Donthi, P.B. Chavan, H. Tan, W. Hennig, A high speed digital data acquisition system for the Indian National Gamma Array at Tata Institute of Fundamental Research Author links open overlay panel. Nucl. Instrum. Methods Phys. Res. A **680**, 90 (2012)
41. D.C. Radford, "ESCL8R and LEVIT8R: Software for interactive graphical analysis of HPGe coincidence data sets", Nucl. Instrum. Methods Phys. Res., Sect. A **361**, 297 (1995)
42. Root-CERN homepage, https://root.cern/
43. M. Rejmund, S. Bhattacharyya, A. Navin, W. Mittig, L. Gaudefroy, M. Gelin, G. Mukherjee, F. Rejmund, P. Roussel-Chomaz, Ch. Theisen, Shell evolution and the $N = 34$ "magic number. Phys. Rev. C **76**, 021304 (2007)
44. J. Jolie, S. Heinze, Level dynamics of non-yrast states. AIP Conf. Proc. **819**, 331 (2006)
45. D. Dell'Aquila, S. Sweany, K.W. Brown, Z. Chajecki, W.G. Lynch, F.C.E. Teh, C.-Y. Tsang, M.B. Tsang, K. Zhu, C. Anderson, A. Anthony, S. Barlini, J. Barney, A. Camaiani, G. Jhang, J. Crosby, J. Estee, M. Ghazali, F. Guan, O. Khanal, S. Kodali, I. Lombardo, J. Manfredi, L. Morelli, P. Morfouace, C. Niu, G. Verde, Non-linearity effects on the light-output calibration of light charged particles in CsI(Tl) scintillator crystals. Nucl. Instrum. Methods Phys. Res. A **929**, 162 (2019)
46. Y. Dong, H. Junde, Nuclear data sheets for A = 54. Nucl. Data Sheets **121**, 1 (2014)
47. Ian J. Thompson, Filomena M. Nunes, *Nuclear Reactions for Astrophysics* (Cambridge University Press, New York, 2009)
48. J. Cook, Global optical-model potentials for the elastic scattering of ^{6,7}Li projectiles. Nucl. Phys. A **388**, 153 (1982)
49. D.R. Tilley, C.M. Cheves, J.L. Godwin, G.M. Hale, H.M. Hofmann, J.H. Kelley, C.G. Sheu, H.R. Weller, Energy levels of light nuclei A=5, 6, 7. Nucl. Phys. A **708**, 3 (2002)
50. C.W. Towsley, D. Cline, R.N. Horoshko, Quadrupole moments and the structure of the even titanium and chromium nuclei. Nucl. Phys. A **250**, 381 (1975)
51. Xiaohua Li, Chuntian Liang, Chonghai Cai, Global triton optical model potential. Nucl. Phys. A **789**, 103 (2007)
52. B. Buck, A.C. Merchant, Cluster model of A=7 nuclei revisited, and the astrophysical S factors for ^{3}He(α,γ)^{7}Be and ^{3}H(α,γ)^{7}Li at zero energy. J. Phys. G Nucl. Phys. **14**, L211 (1988)
53. T. Yoshimura, A. Okihana, R.E. Warner, N.S. Chant, P.G. Roos, C. Samanta, S. Kakigi, N. Koori, M. Fujiwara, N. Matsuoka, K. Tamura, E. Kubo, K. Ushiro, Alpha spectroscopic factors for ^{6}Li, ^{7}Li, ^{9}Be and ^{12}C from the (p, pα) reaction at 296 MeV. Nucl. Phys. A **641**, 3 (1998)
54. R.O. Akyuz, A. Winther, Proc. Enrico Fermi Int. School of Physics, 1979. In: R.A. Broglia et al. (ed.) Nuclear structure and heavy-ion reactions. North-Holland (1981)
55. T. Yamaya, M. Saitoh, M. Fujiwara, T. Itahashi, K. Katori, T. Suehiro, S. Kato, S. Hatori, S. Ohkubo, Cluster structure in ^{40}Ca via the α-transfer reaction. Nucl. Phys. A **573**, 154–172 (1994)
56. H. Faraggi, M.-C. Lemaire, J.-M. Loiseaux, M.C. Mermaz, A. Papineau, Experimental Evidence for Quartet Structure in Cr and Ti Isotopes. Phys. Rev. C **4**, 1375 (1971)